Shape and Motion of a Ruck in a Rug

John M. Kolinski, Pascale Aussillous, and L. Mahadevan*

*School of Engineering and Applied Sciences, Harvard University, Cambridge, Massachusetts 02138, USA
and IUSTI CNRS UMR 6595, Polytech' Marseille, Aix-Marseille Universite, Marseille cedex 13, France*
(Received 21 June 2009; published 21 October 2009)

The motion of a ruck in a rug is used as an analogy to explain the role of dislocations in crystalline solids. We take literally one side of this analogy and study the shape and motion of a bump, wrinkle or ruck in a thin sheet in partial contact with a rough substrate in a gravitational field. Using a combination of experiments, scaling analysis and numerical solutions of the governing equations, we quantify the static shape of a ruck on a horizontal plane. When the plane is inclined, the ruck becomes asymmetric and moves by rolling only when the inclination of the plane reaches a critical angle, at a speed determined by a simple power balance. We find that the angle at which rolling starts is larger than the angle at which the ruck stops; i.e., static rolling friction is larger than dynamic rolling friction. We conclude with a generalization of our results to wrinkles in soft adherent extensible films.

To understand how dislocations in crystalline materials allow for slip along lattice planes, an oft-used analogy, attributed to Orowan [1], connects the motion of a dislocation to that of a ruck in a rug. Just as it is easier to move a rug by having a wrinkle or ruck roll through it rather than by dragging it, it is easier for a crystal to deform by having a dislocation glide or climb rather than having an entire plane of atoms move. However this analogy does not translate literally since a ruck in a rug does not have a quantized Burgers vector, nor is it amenable to a simple elastic treatment that the far field of a dislocation is. Nevertheless, rucks in rugs are inherently interesting objects, and often appear in various guises at soft interfaces. For example, motion at a rubber-glass interface occurs not by sliding but via the generation and propagation of small wrinkles [2]. Similarly, in thin films and filaments that interact with a substrate frictionally or adhesively, motion occurs via the rolling of wrinkles [3,4]. In flagellar axonemes individual microtubules often slide relative to each other via the motor-driven propagation of microscopic wrinkles [5], while in animal cells, blebs, which are blisters where the cell membrane is detached from the underlying cortex, also propagate like rucks [6]. Finally inchworms and their relatives move using propagating wrinkles [7], and very likely played a role in the genesis of the analogy.

Motivated by these studies, we consider the statics and dynamics of a ruck in a thin film of material such as latex, lying on a rough plane, shown in Fig. 1(a) (latex thickness $h = 0.25$ mm), complementing earlier work [8–11] on the shape of a heavy elastic filament on a substrate by using a combination of experimental, scaling and numerical approaches. Assuming that the ruck is inextensible, the instantaneous position of material points in the ruck $x(s, t)$, $y(s, t)$ parametrized using the arc length s and the orientation of the local tangent vector $\phi(s, t)$ relative to the rug plane are related via the kinematic relations

$$\partial_s x = \cos\phi, \qquad \partial_s y = \sin\phi. \tag{1}$$

Here $\partial_a A \equiv \partial A / \partial a$. Force balance parallel and perpendicular to the plane yields the equations of motion [see Fig. 1(b) for a pictorial derivation]:

$$\partial_s F_1 + \rho g h \sin\theta + f_1 = \rho_s \partial_{tt} x,$$
$$\partial_s F_2 - \rho g h \cos\theta + f_2 = \rho_s \partial_{tt} y \tag{2}$$
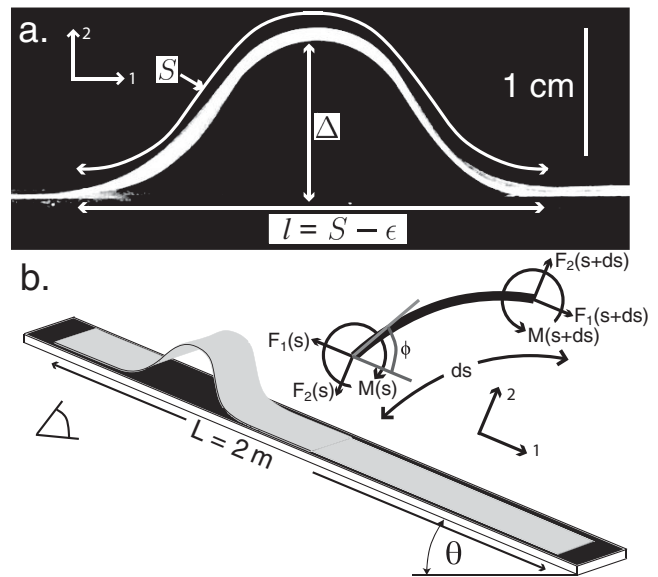$$\partial_s M - F_1 \sin\phi + F_2 \cos\phi + m = 0.$$

FIG. 1. (a) A ruck in a thin latex rug on a flat substrate, of height Δ, length measured along the arc S and horizontal extent $S - \epsilon$. Here ϵ is analogous to the Burgers vector. (b) A schematic shows the ruck on a plane at an angle of inclination θ. The upper right hand corner shows the local stress and moment resultants for a segment of length ds, where ϕ is the angle between the local ruck tangent and the plane.

Here F_1 and F_2 are the integrated stress resultants in the film of density ρ, M is the torque resultant and g is the gravitational acceleration, and f_1, f_2, m are the volumetric body forces and torques at a cross section (including the effects of air drag, etc.) [12]. Closure of the system of equations requires specification of the torque M. Latex rubber is a viscoelastic material which we model as a simple Voigt solid, so that we can write $M = EI_a \partial_s \phi + \mu I_a \partial_{st}^2 \phi$, where I_a is the area moment of inertia of the cross section, E is the elastic modulus and μ is the viscosity of the material. Finding the shape of either the static or dynamic ruck requires the specification of boundary conditions at the two contact lines that demarcate the locations where the ruck leaves and regains contact with the substrate, and read

$$x(0) = y(0) = \phi(0) = \partial_s \phi(0) = y(S) = \phi(S) = 0. \quad (3)$$

Here S is the freely suspended length of the ruck, and the origin of the ruck has been chosen to be the left contact line. Without adhesion, the curvature vanishes at either end, which follows from the absence of localized torques at the contact lines [13].

For small amplitude rucks, the excess length $\epsilon \ll S$, and the projected length of the ruck $l \sim S$. Then the ruck height $\Delta \sim \sqrt{\epsilon l}$, and the ruck curvature $\kappa \sim \Delta/l^2$. Comparing the elastic bending energy, $U_e \sim EI\kappa^2 l$, with the gravitational potential energy, $U_g \sim \rho g h l \Delta$, together with the geometric relations $\kappa \sim \Delta/l^2$, $I \sim h^3$ yields the dimensional scaling laws $l \sim \epsilon^{1/7}(Eh^2/\rho g)^{2/7}$, $\Delta \sim \epsilon^{4/7}(Eh^2/\rho g)^{1/7}$ so that the dimensional energy per unit length of the ruck is $\rho g h \ell_g^{9/7} \epsilon^{5/7}$. Using the elastic gravity length, $\ell_g = (\frac{Eh^2}{\rho g})^{1/3}$ as a natural length scale in the problem then allows us to write the dimensionless length and height of the ruck as

$$l/\ell_g \sim \epsilon^{1/7}, \qquad \Delta/\ell_g \sim \epsilon^{4/7}. \quad (4)$$

For rucks of large amplitude, we must solve the free boundary problem (1)–(3) in the static limit (with $f_1 = f_2 = m = \partial_{tt}x = \partial_{tt}y = 0$). We normalize all lengths by the elastic gravity length, $\ell_g = (\frac{EI_a}{\rho h g})^{1/3}$, stresses by $N = \rho g h \ell_g$, to obtain the dimensionless variables $\hat{x} = x/\ell_g$, $\hat{F}_1 = F_1/N$, $\hat{\epsilon} = \epsilon/\ell_g$, etc., but will drop the hats from now on. Solving (1)–(3) using a shooting method implemented in MATLAB allows us to determine the dimensionless height Δ as a function of the dimensionless excess length ϵ. In Fig. 2(a) we show that the resulting curve agrees very well with the experimentally determined height of the ruck. In Fig. 2(b), we show that the complete shape of the ruck for various values of ϵ, determined experimentally and numerically also agree well [14].

When the plane on which the ruck is formed is tilted, the ruck becomes asymmetric, but does not move. Following along our earlier argument results in the dimensionless length of the ruck $l/\ell_g \sim \epsilon^{1/7}(\cos\theta)^{-2/7}$ and the dimensionless height $\Delta/\ell_g \sim \epsilon^{4/7}(\cos\theta)^{-1/7}$, while the dimen-
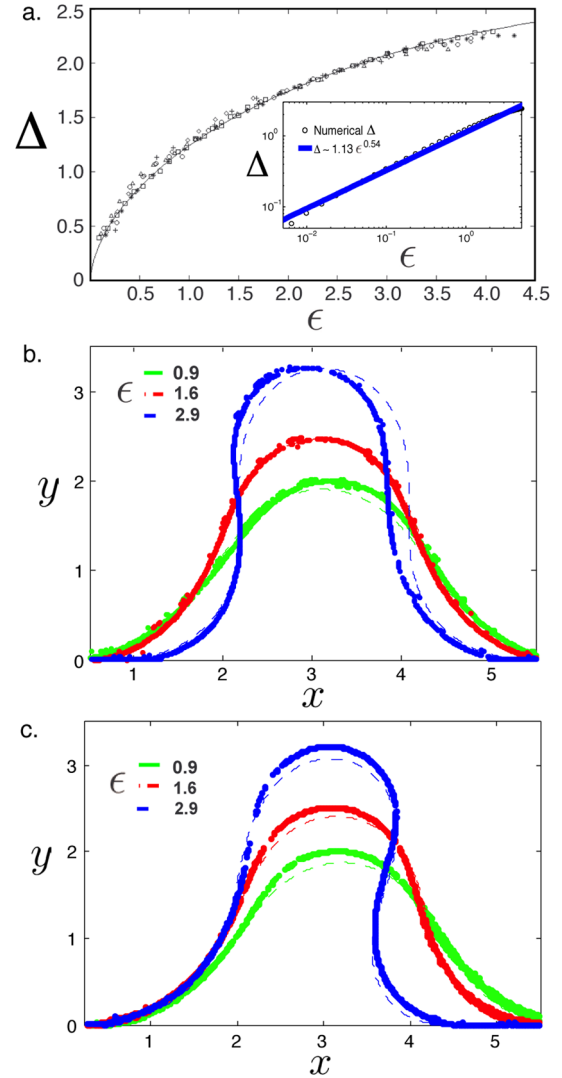

FIG. 2 (color online). (a) The scaled ruck height Δ as a function of the excess length ϵ, for different thicknesses [$h = 0.25$ mm (+), 0.5 mm ($\diamond$), 0.75 mm ($\triangle$), 1.0 mm (*), 1.5 mm ($\bigcirc$)] measured experimentally and calculated numerically by solving (1)–(3) (solid line) collapse onto a single curve. All lengths are normalized by the elastic gravity length, $\ell_g = (\frac{Eh^2}{\rho g})^{1/3}$. The inset shows the numerically calculated values ($\bigcirc$) of Δ as a function of ϵ on a log-log plot and yields a power law $\Delta = \epsilon^{0.54}$ which compares well with the scaling law $\Delta \sim \epsilon^{4/7}$ given by (4). (b) Ruck shape as a function of the excess length, ϵ; the solid lines correspond to experimental measurements, while the dashed lines correspond to numerical solutions of (1)–(3). (c) The ruck shape on an inclined plane with $\sin\theta = 0.3$ shows an increasing asymmetry as ϵ increases. The solid lines correspond to experiments and the dashed lines correspond to numerical solutions of (1)–(3).

sional energy scales as $\rho g h \ell_g^{9/7} \epsilon^{5/7}(\cos\theta)^{4/7}$. To go beyond scaling arguments, we solve the Eqs. (1)–(3) for various values of the tilt θ and excess length ϵ leading to the results shown in Fig. 2(c) along with the experimentally observed shapes, which compare well as long as ϵ is not too large.

When the angle of inclination is larger than a critical threshold, the ruck begins to move. It does so by rolling rather than sliding. Measuring ϵ, the analog of the Burgers vector, at the beginning and the end of the run, we find that it is conserved to within 2%; i.e., there is little slippage during the motion of the ruck. To quantify the rolling motion, we follow the paths of points in the rug that are transported by the ruck. Figure 3(a) shows such a particle path, while the inset shows that it is consistent with the cuspidal profile for a particle on a cycloidal trajectory, well known to characterize the locus of particles on the rim of a circle rolling on a plane. In Fig. 3(b), we show the particle path calculated using a numerical solution of a stationary ruck which compares well with experiments at low tilt angles, when the static and dynamic shape of the ruck are similar to each other.

To determine the critical angle θ_g at which a stationary ruck starts rolling, we tilt the plane smoothly until the ruck moves, wherein it quickly reaches a steady speed V. To determine the angle θ_s at which a steadily moving ruck stops, the incline is untilted slowly (keeping $\partial_t\theta \ll V/S$).

In Fig. 4(a), we see a marked difference between static and dynamic rolling friction characterized in terms of θ_g and θ_s. θ_g is an indicator of a critical torque which a ruck (of a given shape and size) must overcome in order to begin rolling (a measure of static rolling friction), and $\theta_s < \theta_g$ measures dynamic rolling friction, analogous to the well known, but still incompletely understood difference between static and dynamic sliding friction. The existence of a critical inclination for the onset of rolling is similar to the existence of a threshold force for the motion of dislocations [1] in crystals, and thus further extends Orowan's analogy.

When $\theta > \theta_g$, the ruck rolls down at a steady speed V and with a steady shape that is similar to its static shape for small velocities. In Fig. 4(b), we show the variation of V with the inclination θ for different values of ϵ and observe that $V \sim (\sin\theta)^{1/2}$. Since the ruck moves by rolling rather than sliding, the gravitational power must be balanced by either air drag or dissipation within the ruck. In the inset in Fig. 4(b), we see that for ruck speeds of $O(1)$ m/s, the rolling ruck is significantly distorted relative to its static shape, suggesting that air drag is the dominant factor that limits speed. Then, balancing the gravitational power $\rho h l V g \sin\theta$ with the power dissipated by air drag $\rho_f V^3 \Delta$
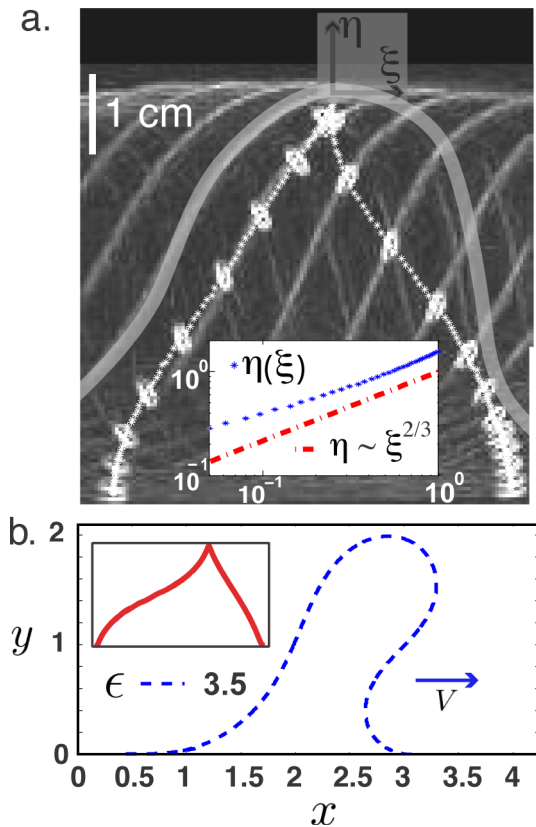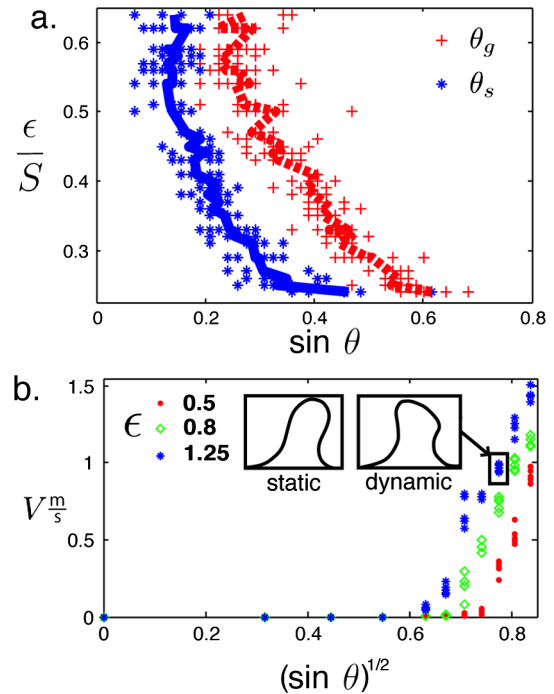

FIG. 3 (color online).   (a) The path of a point on the rug as a ruck (in white *) and time-lapse images of the ruck for $\epsilon = 1.25$, $\theta = 20°$, $V = 0.7$ m/s. The inset shows the path of a point on the ruck as it approaches its zenith (*), compared with the curve $\eta \sim \xi^{2/3}$ that characterizes the trajectory of a point on a cycloidal curve characterizing the rolling of a rigid circle. (b) The numerically calculated shape of a static ruck ($\epsilon = 3.5$, $\theta = 17°$—dashed line), and the path of a point on the rug (inset, solid line) as the ruck moves through it.

FIG. 4 (color online).   (a) The tilt for the onset of rolling θ_g and its arrest θ_s as a function of the shape of the ruck, characterized by the ratio of the excess length to the contour length ϵ/S. Since $\theta_s > \theta_g$ dynamic rolling friction is less than static rolling friction. (b) Ruck speed V vs $\sqrt{\sin\theta}$ when $\theta > \theta_s$ for $\epsilon = 0.5$, 0.8 and 1.25, is consistent with $V \sim \sqrt{\sin\theta}$ (see text). The inset shows the dynamic distortion of the shape of the ruck due to air drag ($\sin\theta = 0.6$, $\epsilon = 1.25$). Velocity experiments used a latex sheet of thickness $h = 0.75$ mm.

yields $V \sim (\rho g h \sin\theta/\rho_f)^{1/2}(\ell_g/\epsilon)^{3/14}$ for small amplitude rucks. Using the parameter values $\rho/\rho_f \sim 10^3$, $h \sim 10^{-3}$ m, $g \sim 10$ m·s^{-2}, $\ell_g/\epsilon \sim 1$ yields $V \sim 5$ m·s^{-1}. To distinguish between the scaling of the speed with $\sin\theta$ and $\sqrt{\sin\theta}$ given the range of θ accessible experimentally, we also decreased the thickness of the sheet by a factor of 3 and found that the terminal velocity decreased by a factor of $1/\sqrt{3} \sim 0.6$ [15]. While the dependence of the speed on the angle of inclination is consistent with our observations, we do not see evidence that smaller rucks are faster than larger ones as predicted by the scaling law. This is likely because small rucks, for which the scaling law is valid, do not move until the angle of inclination is so large that the entire sheet slips before the ruck moves.

Our study has answered the simplest questions about the shape and steady motion of an inextensible ruck in a rug. To go beyond this and understand the transition to rolling in a tilted ruck requires knowledge of the frictional and adhesive interactions at the elastic contact lines which are locally pinned by the asperities that indent the soft but heavy ruck. Then the ruck remains stationary as long as the net torque on the ruck $M_r = EI\partial_s\phi(0) - EI\partial_s\phi(S) + \rho g Slp(\epsilon/S, \theta) < M_c$, where $p(\cdots)$ is a dimensionless function of the shape of the ruck, and the slope of the substrate, and M_c is a threshold torque that depends on the rug-substrate interaction. When $M_r = M_c$, the ruck begins to roll. Similarly, the start-stop rolling hysteresis may be consequence of the fact that the ruck can be pinned to the rough substrate only if the time for adhesion is comparable to the time for the motion of the ruck.

We complete our study with brief consideration of how blisters, rucks and wrinkles can form and move in soft, extensible films that adhere to a substrate, generalizing the analysis of rucks in an inextensible film [4]. Neglecting the effects of gravity, the energy per unit width of the film of length l is $W = U_a + U_b + U_c$, where $U_a \sim Jl$ is the adhesive energy, $U_b \sim Eh^3\epsilon/l^2$ is the bending energy, and $U_c \sim Eh\epsilon^2/l$ is the compressive strain energy. Here, we have assumed that the longitudinal displacement ϵ and the lateral displacement Δ are related by the geometric relation $\Delta \sim (\epsilon l)^{1/2}$. Minimizing $W(\epsilon, l)$ with respect to ϵ, l yields scaling laws for the critical compression $\epsilon_c \sim (Jh^3/E)^{1/4}$ required to create a ruck of a critical size $l_c \sim (Eh^5/J)^{1/4}$. Unlike the inextensible case, the ruck in an extensible film arises via a subcritical instability, analogous to the formation of a bubble in a liquid via a first-order transition; i.e., the ruck when formed has a finite size. These rucks move in an adhesion gradient ∇J. Indeed, balancing the power dissipated in the ruck $\mu h^3(\partial_t\kappa)^2l$ with the driving power ∇JVl shows that the wrinkle speed

$V \sim (h\nabla J/\mu)(Eh/J)^{3/2}$. Specializing these results to various soft systems [4–6] remains a problem for the future.

From a broader perspective, we see that the existence and motion of rucks in rugs generalizes the notion of dislocations in bulk crystals to thin films. Just as glide, climb, etc., correspond to soft modes of a dislocation in a bulk crystal, a localized ruck characterizes the soft modes of a thin film. In either case, the localized structure mediates transitions between different, possibly metastable, states of a system, and undoubtedly there are other examples of this phenomenon waiting to be explored.

Note added.—As this work was being completed, we became aware of [16] which addresses similar questions.

———

*lm@seas.harvard.edu

[1] F. Nabarro, *Theory of Dislocations* (Dover, New York, 1982).
[2] A. Schallamach, Wear **17**, 301 (1971).
[3] J. H. Gittus, Philos. Mag. **31**, 317 (1975).
[4] K. Kendall, Nature (London) **261**, 35 (1976).
[5] S. Aoyama and R. Kamiya, Biophys. J., **89**, 3261 (2005).
[6] G. Charras, T. Mitchison, and L. Mahadevan, Biophys. J. **94**, 1836 (2008).
[7] E. R. Trueman, *Locomotion of Soft Bodied Animals* (Arnold, London, 1975).
[8] J. Flaherty and J. Keller, SIAM J. Appl. Math. **24**, 215 (1973).
[9] C. Y. Wang, Int. J. Mech. Sci. **28**, 549 (1986), and references therein.
[10] S. Santillan, L. Virgin, and R. Plaut, J. Appl. Mech. **73**, 664 (2006).
[11] G. Domokos, W. Fraser, and I. Szeberényi, Physica (Amsterdam) **185D**, 67 (2003).
[12] A. E. H. Love, *A treatise on the Mathematical Theory of Elasticity* (Dover, New York, 1944), 2nd ed..
[13] The condition $\partial_s\phi(S) = 0$ is automatically satisfied as can be verified by multiplying the last equation in (2) by $\partial_s\phi$, and integrating the result.
[14] Beyond a critical excess length ϵ_c, the ruck loses symmetry and tilts to one side [10].
[15] When internal dissipation dominates air drag, balancing the viscoelastic power dissipation $\mu h(h\partial_t\kappa)^2l$, where $\partial_t\kappa \sim V\partial_s\kappa \sim V\Delta/l^3$, with gravitational power input $\rho h l V g \sin\theta$ yields the dimensional speed for small rucks $V \sim \rho g\epsilon^{-2/7}l_g^{30/7}\sin\theta/\mu h^2$. This scaling law might well be relevant for very soft films but is not relevant for our latex sheets.
[16] D. Vella, A. Boudaoud, and M. Adda-Bedia, this issue, Phys. Rev. Lett. **103**, 174301 (2009).